scientific reports

Check for updates

OPEN

Prognostic value of IFI27 in HNSCC and functional analysis under ALKBH5 regulation

Chunxiao Wang[1,2], Zhong Chen[1,2], Tianke Li[1,2], Yang Bao[1,2], Jie Guo[1,2] & Suxin Zhang[1,2]✉

This study aimed to investigate the expression levels and clinical implications of interferon α inducible protein 27 (IFI27) and the N6-methyladenosine (m6A) regulator Alkylation repair homolog 5 (ALKBH5) in head and neck squamous cell carcinoma (HNSCC). We employed bioinformatics methods to analyze the differential expression of IFI27 in HNSCC and its prognostic implications. Additionally, we explored the pathways and mechanisms associated with its enrichment. Immunohistochemistry (IHC) was used to detect the expression of IFI27 protein in HNSCC and adjacent normal tissues. IFI27 expression was significantly up-regulated in HNSCC ($P < 0.001$), and was correlated with T stage and tumor differentiation degree. The survival curve indicated that patients with high IFI27 expression had shorter overall survival compared to those with low expression. Furthermore, multivariate analysis confirmed that IFI27 expression is an independent prognostic factor in HNSCC patients. IFI27 is involved in the regulation of type I and type III interferon-mediated responses, Retinoic acid-inducible gene I (RIG-I) -like receptor signaling pathways, and biological processes related to innate immune responses. High IFI27 expression is a potential risk factor for the onset and progression of HNSCC. Additionally, the down-regulation of ALKBH5 may enhance IFI27 expression via the RIG-I/IFN-α axis, further influencing the development of HNSCC.

Keywords Head and neck squamous cell carcinoma (HNSCC), IFI27, m6A regulators, Immune regulation biomarkers, Immunohistochemistry (IHC), Bioinformatics

Head and neck squamous cell carcinoma (HNSCC) is a prevalent malignancy that significantly impacts patient morbidity and mortality, primarily affecting the oral cavity, oropharynx, larynx, and nasopharynx. HNSCC ranks as the sixth most common cancer globally, with around 600,000 new cases diagnosed annually[1–3]. The incidence of HNSCC is expected to increase by 30% by 2030, which means there will be approximately 1.08 million new cases each year[4]. HNSCC patients experience various levels of functional impairment, including slurred speech and difficulties with eating, at different stages of disease progression and treatment due to the complex anatomy and physiology of the head and face[5]. Moreover, the high recurrence rates of this disease, along with the associated treatment costs, place a significant burden on healthcare systems. Current therapeutic strategies, including surgical resection, radiation therapy and chemotherapy, often yield limited efficacy and are accompanied with considerable adverse effects, underscoring the urgent need for novel biomarkers and therapeutic targets to improve patient outcomes. Recent studies have suggested that specific gene expressions may correlate with HNSCC progression and prognosis, highlighting the potential of molecular markers in enhancing clinical management of this disease.

Interferon-stimulated genes (ISGs) are a collection of genes activated and induced by interferons (IFNs) via the Janus kinase (JAK) and Signal transducer and activator of transcription (STAT) pathways[6]. This collection includes over 300 genes, among which is the ISG12 gene set. The IFI27 gene, also known as ISG12a, located on human chromosome 14q32[7], is a small hydrophobic mitochondrial protein composed of 122 amino acids[8], which is considered to be a mitochondrial matrix protein due to its localization in the mitochondria[9]. IFI27 is one of the genes most strongly induced by Type I interferon (IFN-I)[10]. Recent studies have indicated that IFI27 is involved in several biological processes, including innate immune regulation and epithelial-mesenchymal transition, both of which are linked to the onset and progression of various cancers. Furthermore, the involvement of IFI27 in immune responses and its interaction with pathways such as NF-κB suggests that it may play a critical role in tumor immune evasion and microenvironment modulation, although its specific mechanisms in HNSCC remain inadequately characterized[11].

[1]Department of Stomatology, The Fourth Hospital of Hebei Medical University, Shijiazhuang 050011, People's Republic of China. [2]Hebei Key Laboratory of Stomatology, Hebei Medical University, Shijiazhuang 050017, People's Republic of China. ✉email: jasmine@hebmu.edu.cn

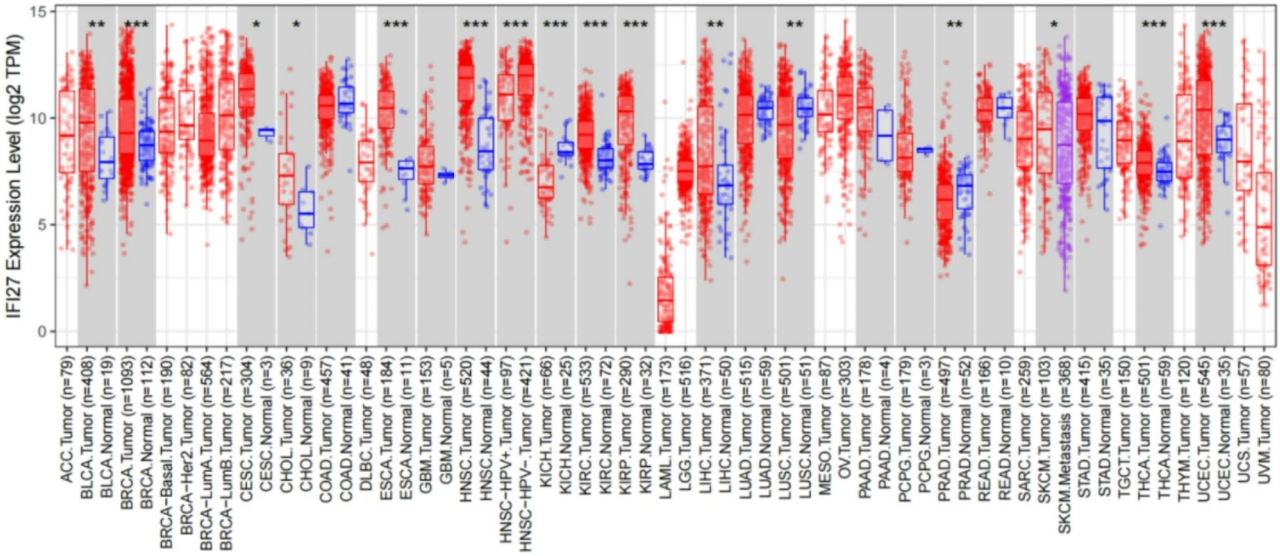

Fig. 1. Expression of IFI27 in pan-cancer tissue in the TIMER 2.0 database (Note: * $P<0.05$; ** $P<0.01$; *** $P<0.001$, red: tumor tissue, blue: normal tissue).

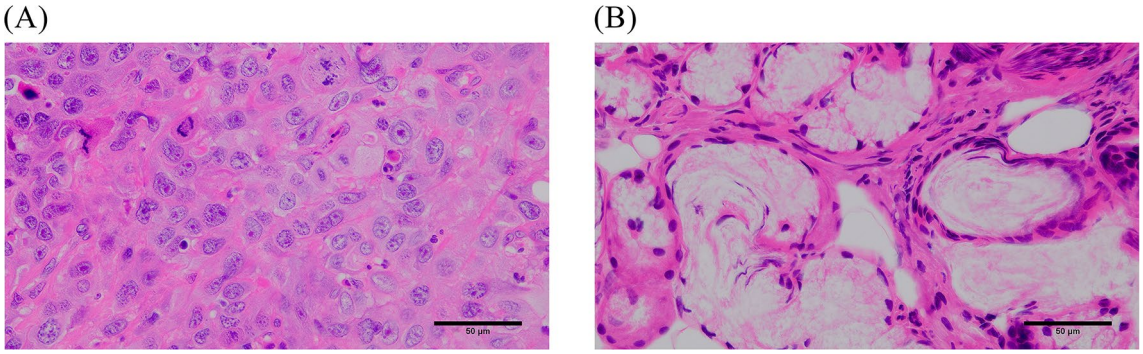

Fig. 2. HE staining of cancer tissue and normal tissue. (A) HE staining of cancer tissue (10×40). (B) HE staining of normal tissue (10× 40).

The m6A modification is a widely occurring change in mRNA that impacts various processes in RNA metabolism, such as splicing, translation, and degradation[12], it is also dynamic and reversible. This process includes methyltransferases (known as 'writers'), demethylases ('erasers'), and binding proteins ('readers')[13]. These components can simultaneously activate various oncogenic signaling pathways[14]. The ALKBH5 gene, a demethylase that recognizes m6A modification on RNA, has been shown to play a role in the development of several types of cancer, including glioma, pancreatic cancer, gastric cancer, and non-small cell lung cancer[15–18].

Although there is increasing evidence of the importance of IFI27 and ALKBH5 in cancer biology, their specific roles in HNSCC remain unclear. Our research aims to explore the relationship between IFI27 and clinical features of HNSCC, including overall survival (OS) and its effect in HNSCC pathogenesis, and the relationship between IFI27 and ALKBH5. We achieve this by analyzing publicly available datasets, particularly from The Cancer Genome Atlas (TCGA), in conjunction with Immunohistochemistry (IHC).

Results

IFI27 expression was significantly up-regulated in HNSCC tissues

According to the TIMER 2.0 database, IFI27 expression is significantly elevated in various cancers, such as HNSCC, bladder cancer, esophageal squamous cell carcinoma, renal clear cell carcinoma, and endometrial carcinoma (Fig. 1). HE staining was performed on the tumor tissue and the adjacent tissue, which confirmed that the adjacent tissue was normal tissue (Fig. 2A, B). The IHC results from 57 clinical cases demonstrated that IFI27 is predominantly expressed in the nucleus and mitochondria, with positive staining varying from light yellow to brown (Fig. 3A, B). A comparison of IFI27 expression was conducted between HNSCC and adjacent normal tissues from the 57 clinical cases. This analysis revealed a significant difference ($P<0.001$) (Fig. 3C).

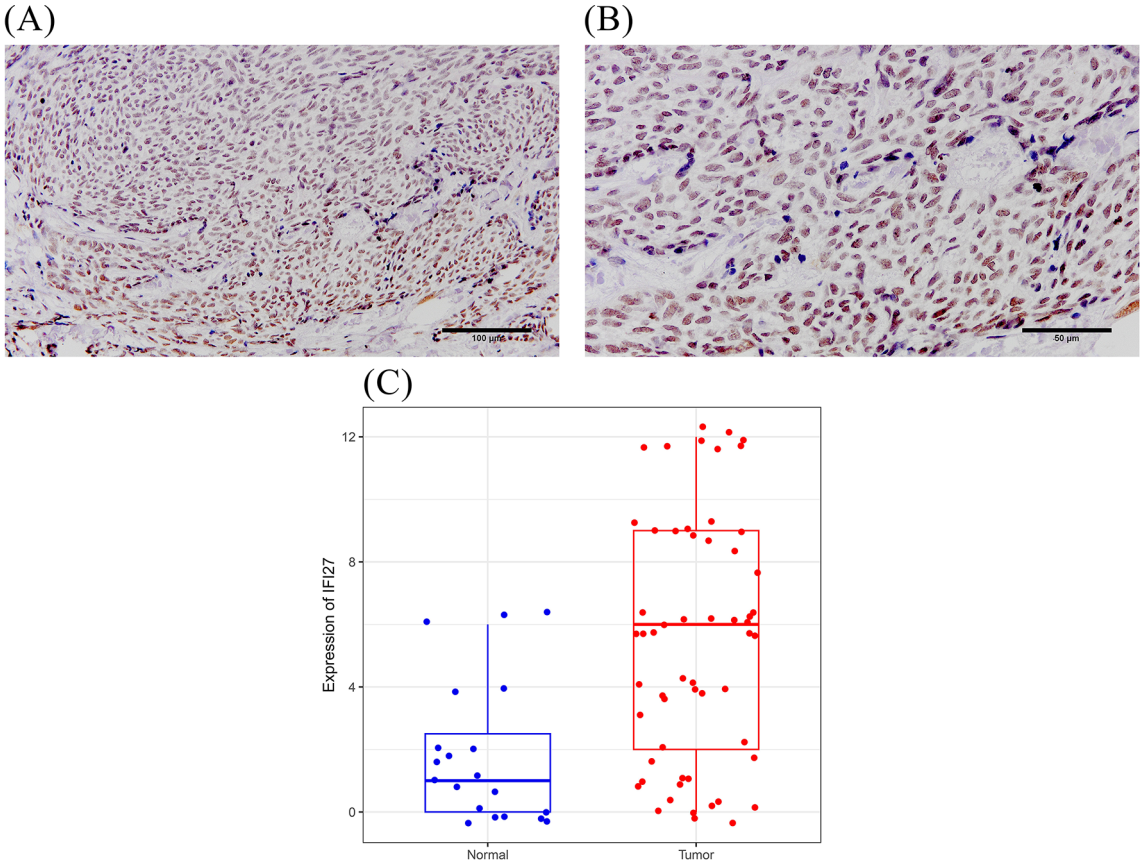

Fig. 3. Expression of IFI27 in HNSCC. (A) IHC staining of IFI27 in HNSCC (10 × 20). (B) IHC staining of IFI27 in HNSCC (10 × 40). (C) Differential expression of IFI27 in HNSCC and adjacent normal tissues ($P < 0.001$).

The relationship between the expression of IFI27 and the clinicopathological features of HNSCC

In the UALCAN database, IFI27 expression was significantly correlated with tumor differentiation, gender, and promoter methylation, but showed no correlation with age, lymph node metastasis, or TNM stage (Fig. 4). The Chi-square test of IHC results from 57 clinical cases indicated that IFI27 expression correlated with T stage ($P = 0.028$) and tumor differentiation ($P = 0.003$) in HNSCC patients. However, it showed no correlation with age, gender, N stage, TNM stage, smoking, or alcohol consumption (Table 1).

The relationship between the expression of IFI27 and the prognosis of HNSCC

The Kaplan-Meier (KM) curve for 409 patients in the TCGA database showed that those with high IFI27 expression had a shorter OS of 601 days (Median survival) compared to 740.5 days for patients with low IFI27 expression ($P = 0.033$) (Fig. 5A). Univariate analysis indicated that age, T stage, N stage, TNM stage and IFI27 expression were associated with poor prognosis in HNSCC, while multivariate analysis identified age, T stage, N stage, and IFI27 expression as independent prognostic factors (Table 2).

The KM curve for 57 clinical cases revealed that patients with high IFI27 expression had an OS of 753 days, which was shorter than the 842 days for those with low IFI27 expression ($P = 0.029$) (Fig. 5B). Univariate analysis indicated that N stage, TNM stage, and IFI27 expression were linked to poor prognosis in HNSCC, while multivariate analysis confirmed that IFI27 expression was an independent prognostic factor (Table 3).

GO and KEGG enrichment analysis of IFI27-related expression genes

The GO and KEGG[19–21] pathway enrichment analysis of the gene sets containing IFI27 and its related genes (Fig. 6) revealed several biological processes associated with IFI27, including the defense response to virus, negative regulation of viral life cycle, and response to IFN-I. Additionally, the relevant cellular components encompassed the cytoplasmic vesicle lumen, proteasome core complex, and canonical inflammasome complex. The molecular functions identified were binding to single/double-stranded RNA and nucleotidyltransferase activity. Finally, the KEGG pathways highlighted included the NOD-like receptor signaling pathway, cytosolic DNA-sensing pathway, and RIG-I-like receptor signaling pathway. The abundant GO terms and KEGG pathways suggest that IFI27 and its related genes play a significant role in promoting cytokine production, participating in the innate immune response, and inducing inflammatory responses and apoptosis (programmed cell death).

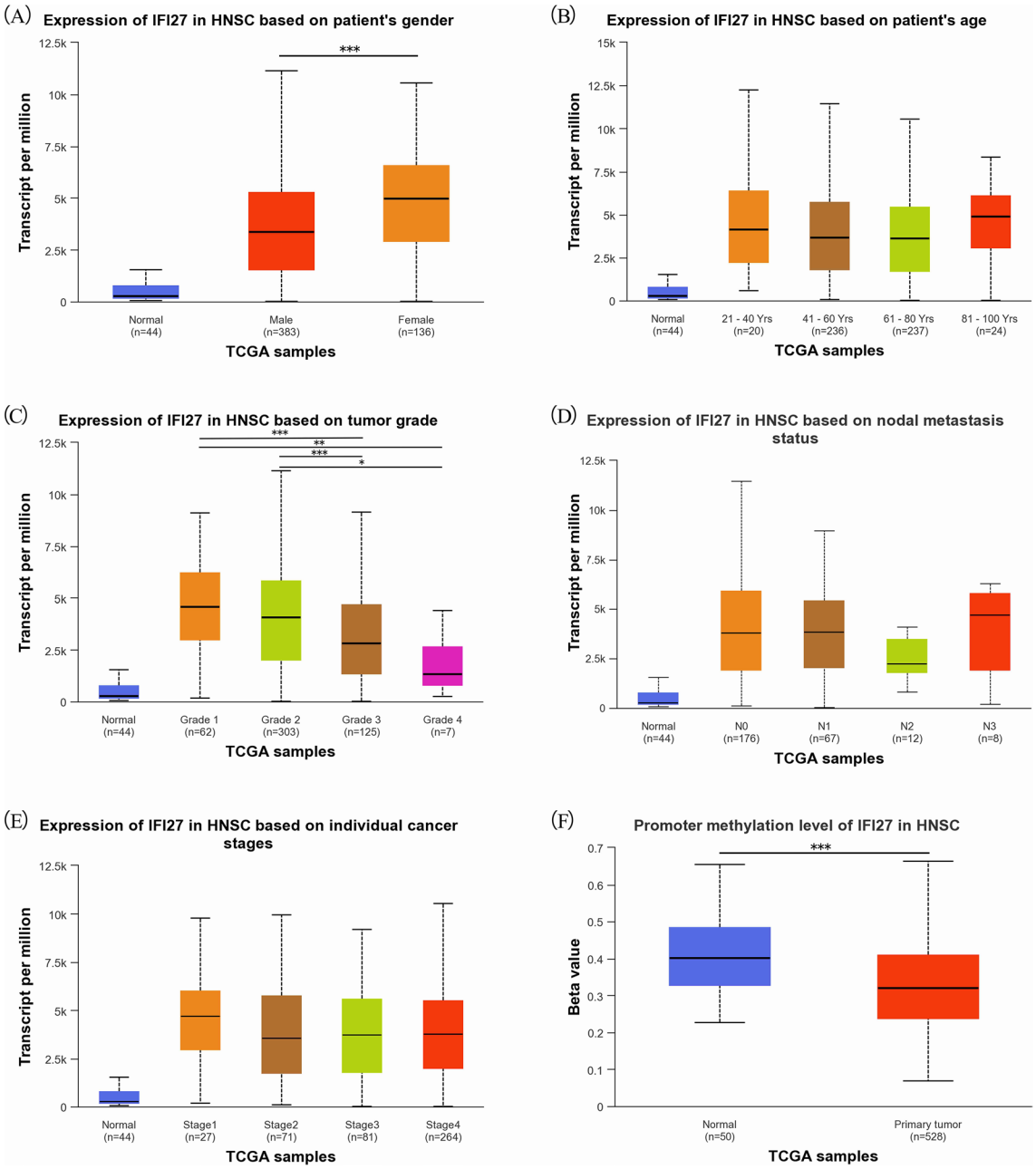

Fig. 4. The relationship between IFI27 and the clinicopathological features of HNSCC patients in UALCAN. (A) Patient's gender. (B) Patient's age. (C) Tumor grade. (D) Nodal metastasis. (E) Cancer stages. (F) Promoter methylation (Note: * $P<0.05$; ** $P<0.01$; *** $P<0.001$).

These processes are closely linked to the occurrence and development of malignant tumors, indicating their potential importance in HNSCC formation and progression.

GSEA of IFI27-related DEGs

Based on the TCGA database, we identified 6,355 differentially expressed genes (DEGs). Through Gene Set Enrichment Analysis (GSEA), we found that 14 gene sets were significantly enriched (Fig. 7). According to the normalized enrichment score (NES), these gene sets were categorized into eight that showed an up-regulated trend and six that showed a down-regulated trend.

The gene sets showing an up-regulated trend included: IFN-α response, E2F targets, IFN-γ response, G2M checkpoint, Epithelial mesenchymal transition, Mitotic spindle, MYC targets v1, Inflammatory response. The down-regulated gene sets included Myogenesis, Adipogenesis, Fatty acid metabolism, Estrogen response early, Oxidative phosphorylation, and KRAS signaling dn.

Characteristics	*n*	IFI27 expression		χ^2	*P*
		High	Low		
Age (years)				0.154	0.695
≥70	10	6	4		
<70	47	25	22		
Gender				0.321	0.571
Male	33	19	14		
Female	24	12	12		
T stage				4.859	0.028*
T1–T2	35	15	20		
T3–T4	22	16	6		
N stage				0.758	0.384
N0	36	18	18		
N+	21	13	8		
TNM stage				1.222	0.269
I–II	24	11	13		
III–IV	33	20	13		
Tumor grade				8.717	0.003*
G1–G2	45	29	16		
G3	12	2	10		
Smoking				0.491	0.483
Yes	27	16	11		
No	30	15	15		
Alcohol consumption				0.888	0.346
Yes	28	17	11		
No	29	14	15		

Table 1. 57 clinical cases of IFI27 expression and clinical pathological characteristics of HNSCC patients (* $P < 0.05$).

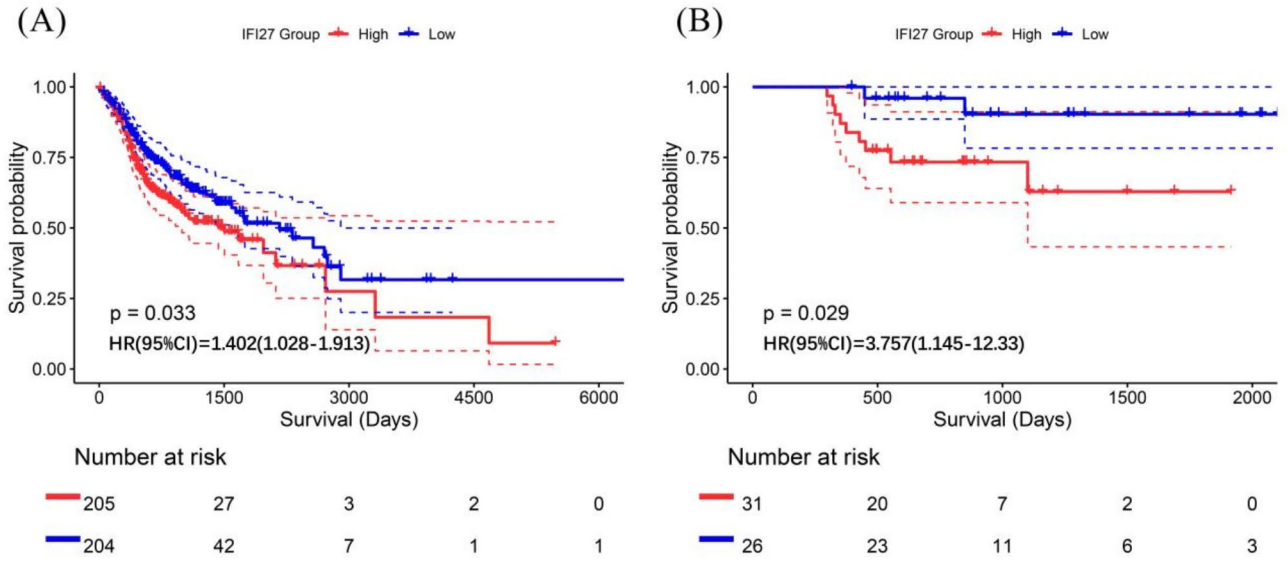

Fig. 5. Influence of IFI27 expression difference on OS in HNSCC patients. (A) KM curve for 409 patients from TCGA database. (B) KM curve for 57 clinical cases.

Co-expression analysis of IFI27 and m6A modification-related regulatory factors

We analyzed the expression levels of 23 m6A modification-related regulatory factors in the high-expression and low-expression groups of IFI27 (Fig. 8). In the IFI27 low-expression group ($n = 204$), six m6A modification-related regulatory factors (RBM15B, CBLL1, ALKBH5, IGF2BP3, LRPPRC, ELAVL1) were significantly over-

Characteristics		n	Univariate analysis		Multivariate analysis	
			HR (95% CI)	P	HR (95% CI)	P
Age(years)	≥70	77	1.666 (1.163–2.387)	0.005*	1.907 (1.327–2.740)	<0.0001*
	<70	332				
Gender	Male	303	0.745 (0.532–1.044)	0.087		
	Female	106				
T stage	T1–T2	148	2.303 (1.584–3.350)	<0.0001*	2.137 (1.328–3.440)	0.002*
	T3–T4	261				
N stage	N0	171	1.880 (1.346–2.625)	<0.0001*	1.770 (1.202–2.608)	0.004*
	N+	238				
TNM Stage	I–II	75	2.784 (1.609–4.816)	<0.0001*	1.080 (0.495–2.356)	0.847
	III–IV	334				
Smoking	Yes	235	0.944 (0.691–1.290)	0.719		
	No	174				
Alcohol consumption	Yes	268	1.010 (0.725–1.405)	0.955		
	No	133				
IFI27 expression	High	205	1.400 (1.026–1.910)	0.034*	1.370(1.004–1.868)	0.047*
	Low	204				

Table 2. Cox analysis of 409 patients in TCGA (HR, hazard ratio; 95%CI, 95% confidence interval; * $P<0.05$).

Characteristics		n	Univariate analysis		Multivariate analysis	
			HR (95% CI)	P	HR (95% CI)	P
Age(years)	≥70	10	1.773 (0.468–6.709)	0.399		
	<70	47				
Gender	Male	33	0.956 (0.291–3.143)	0.941		
	Female	24				
T Stage	T1–T2	35	2.405 (0.727–7.956)	0.150		
	T3–T4	22				
N Stage	N0	36	3.588 (1.047–12.288)	0.042*	1.653(0.422–6.478)	0.471
	N+	21				
TNM Stage	I–II	24	8.489(1.084–66.446)	0.042*	6.145 (0.636–59.389)	0.117
	III–IV	33				
Smoking	Yes	27	0.719 (0.210–2.456)	0.600		
	No	30				
Alcohol consumption	Yes	28	0.918 (0.280–3.011)	0.888		
	No	29				
IFI27 expression	High	31	4.739 (1.018–22.066)	0.047*	4.886(1.018–23.436)	0.047*
	Low	26				

Table 3. Cox analysis of 57 clinical cases of HNSCC (HR, hazard ratio; 95%CI, 95% confidence interval; * $P<0.05$).

expressed compared to the high-expression group ($n=205$) ($P<0.05$). Additionally, the expression of HNRNPC, another m6A modification-related regulatory factor, was significantly lower in the low-expression group ($P<0.05$).

Discussion

HNSCC consists of diverse malignant tumors influenced by various factors. The incidence of HNSCC is typically 2–4 times higher in male than in female. Individuals who smoke heavily and consume alcohol have a risk of developing HNSCC that is over 35 times greater[22]. Persistent HPV infection is a risk factor for oropharyngeal cancer, while EBV is associated with nasopharyngeal cancer[2324]. Additionally, individuals with certain genetic factors, such as Fanconi anemia, are 500–700 times more likely to develop HNSCC compared to the general population[25].

Many patients are diagnosed at an advanced stage[26]. Currently, HNSCC treatment primarily involves surgical resection, supplemented by radiotherapy and chemotherapy. However, these therapies mainly target residual tumor tissue and often result in severe, intolerable side effects. Recently, non-invasive immunotherapy has emerged as an exciting frontier in cancer treatment, increasingly complementing traditional therapies. However,

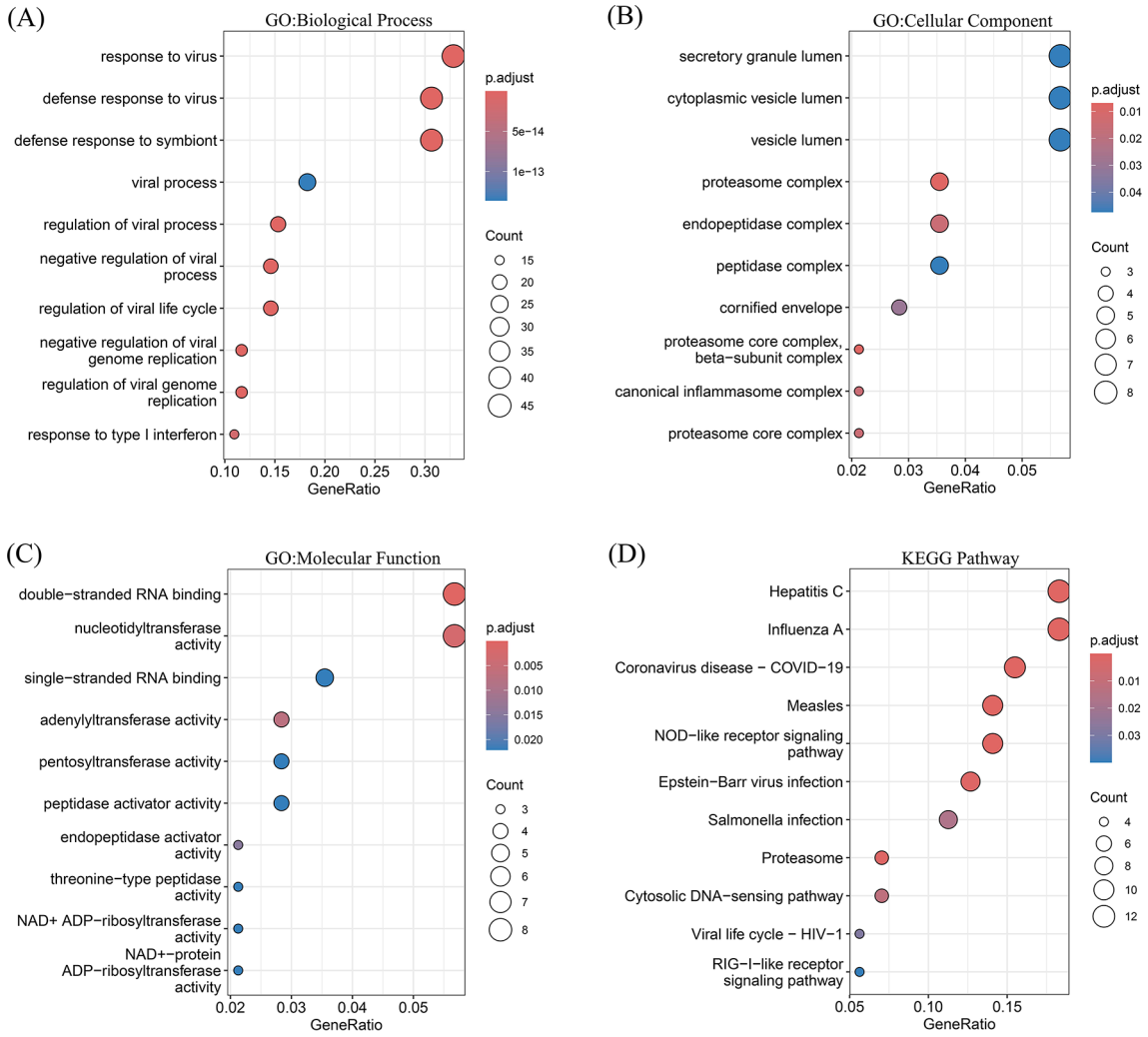

Fig. 6. GO and KEGG enrichment analysis of IFI27-related genes. (A) GO: Biological Process, (B) GO: Cellular Component, (C) GO: Molecular Function, (D) KEGG Pathway.

in the context of highly immunosuppressive HNSCC, identifying the patient population that would benefit from treatment and addressing drug resistance remain significant challenges. Therefore, exploring new therapeutic targets and predictors to improve the survival rate of HNSCC patients is still a hot topic in this field.

The initiation of the innate immune response relies on pattern recognition receptors, including RIG-I-like receptors, NOD-like receptors, and DNA sensors[27]. These receptors are the first responders to abnormal cells[28], such as tumor cells, triggering the activation of downstream signaling pathways that produce proinflammatory cytokines, including IFNs. IFNs induce the production of ISGs through a series of signaling events, ISGs and their expression products can regulate IFNs signaling pathways positively or negatively, exerting immune regulatory functions[29]. IFI27, a member of the ISG12 gene family, is an innate immune effector molecule, and the family of ISGs involved in mediating the innate immune response serves as the first line of defense against cancer. However, recent reports have identified IFI27 as an oncogene, which is up-regulated in various cancers and associated with poor survival rates. At present, the role of IFI27 in the occurrence and development of HNSCC remains to be further explored.

Our analysis of the TCGA database revealed that IFI27 is up-regulated in various cancers, including HNSCC. We also found that the expression of IFI27 was associated with gender and tumor differentiation. Immunohistochemistry analysis of 57 clinical cases showed significant differences in IFI27 expression between HNSCC and adjacent normal tissues. Furthermore, the expression of IFI27 was correlated with T stage and tumor differentiation, suggesting that the over-expression of IFI27 contributes to the progression of HNSCC. We discovered that the level of IFI27 promoter methylation in HNSCC tumor tissues was significantly lower compared to normal tissues. Research indicates that gene methylation plays a crucial role in genomic epigenetic modification. Hypomethylation can lead to genomic instability and activate gene transcription, which is closely linked to tumor development[30]. Therefore, we hypothesize that HNSCC may promote the over-expression of IFI27 by down-regulating the methylation of its promoter.

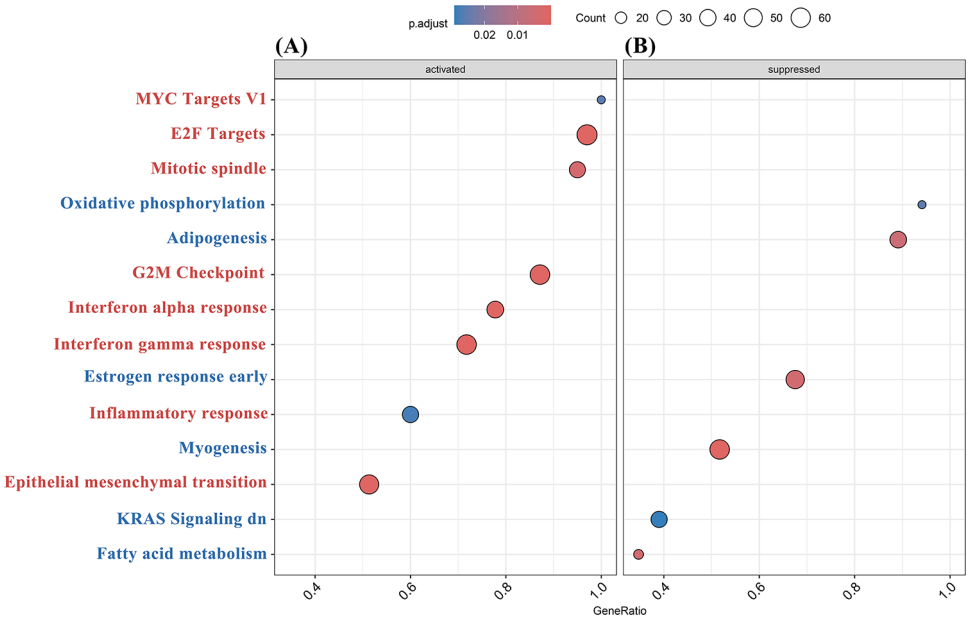

Fig. 7. GSEA enrichment analysis of IFI27-related DEGs. (A, B) Up-regulated and down-regulated gene sets resulting from the enrichment of IFI27-related DEGs. (Red: up-regulated gene sets, blue: down-regulated gene sets)

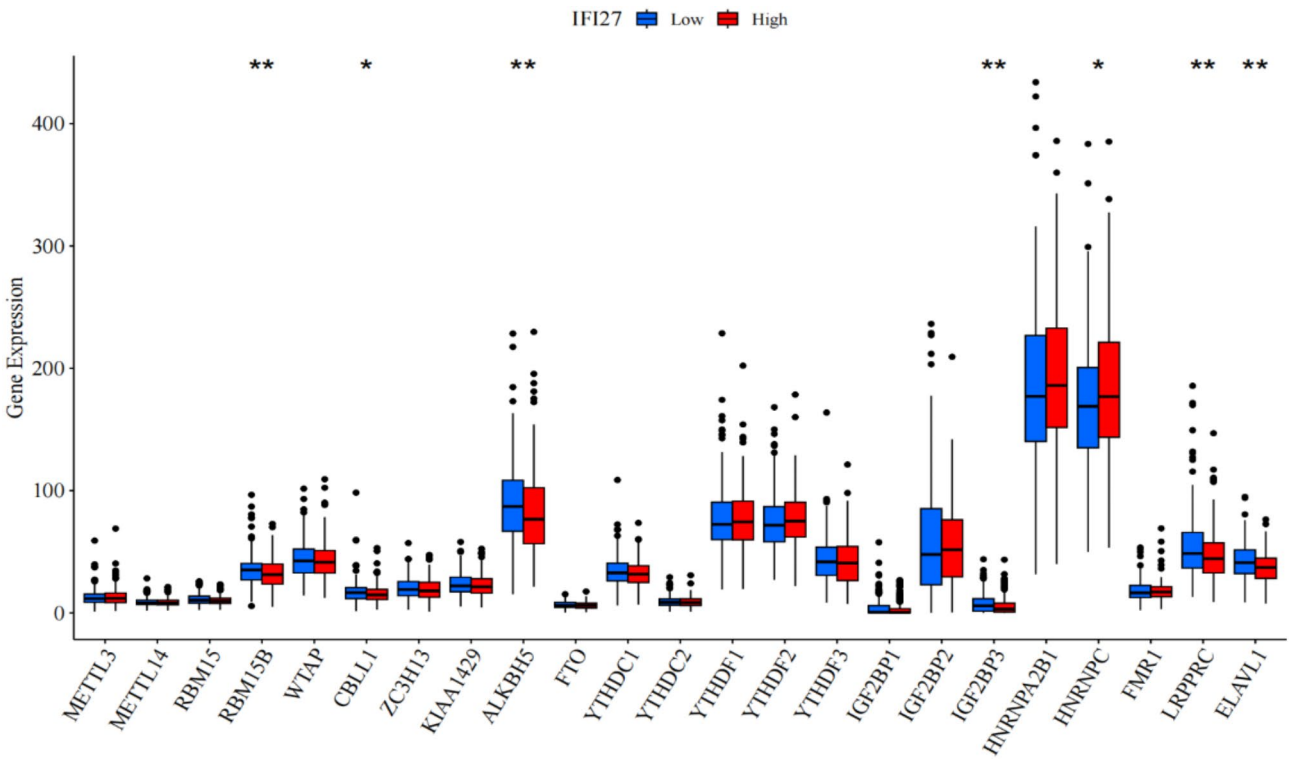

Fig. 8. The relationship between IFI27 expression and 23 m6A modification-related regulatory factors. (Note: * $P<0.05$; ** $P<0.01$; *** $P<0.001$)

We further explored the relationship between IFI27 expression levels and the prognosis of HNSCC using the TCGA database. The results indicated that patients with high IFI27 expression had shorter OS compared to those with low expression. COX regression analysis showed that age, T stage, N stage, and IFI27 expression were independent prognostic factors affecting patients with HNSCC. Subsequently, we verified these conclusions using immunohistochemical expression results from 57 clinical cases, and the survival analysis was consistent with

our analysis in the TCGA database. COX regression analysis showed that IFI27 expression was an independent prognostic factor affecting HNSCC patients. Our findings suggest that IFI27 may serve as a biomarker for predicting poor prognosis in HNSCC.

We explored the mechanism of IFI27 in HNSCC using GO, KEGG, and GSEA. The results indicated that IFI27 was involved in regulating IFN-I (IFN-α) and IFN-γ mediated responses, the RIG-I-like receptor signaling pathway, promoting inflammatory response, and other biological processes related to innate immune response, which can also induce epithelial-mesenchymal transition (EMT).Studies have found that IFI27, a protein highly induced by IFN-I, interfered with RIG-I signaling and affected RIG-I activation by binding to single/double-stranded RNA, thereby negatively regulating innate immune responses[31]. EMT leads to cells losing epithelial markers and gaining mesenchymal markers. Recent reports have highlighted that IFI27 is significantly over-expressed in human ovarian cancer and cholangiocarcinoma, and is associated with poor tumor prognosis. IFI27 promotes the growth and metastasis of ovarian and cholangiocarcinoma by inducing EMT[3233]; $CD8^+$ T cells can eliminate transformed tumor cells and regulate immune responses, but in pancreatic cancer, high expression of IFI27 reduces the degree of $CD8^+$ T cell infiltration, thereby weakening its immune effect[34]. By combining our functional enrichment analysis from the TCGA database with other studies on IFI27 in malignant tumors, we further infer that IFI27 may facilitate tumor progression. It may promote the occurrence and development of HNSCC by negatively regulating innate immune responses and inducing EMT in the tumor microenvironment. We believe that further evaluation of IFI27 as a therapeutic target for HNSCC is warranted.

As an important member of m6A modification, ALKBH5 plays an indispensable role in cancer development. In human non-small cell lung cancer, ALKBH5 decreases tumor growth, invasion, and metastasis by reducing YES-associated protein levels in the m6A-mediated Hippo signaling pathway[18]. In HNSCC, RIG-I protein is encoded by DDX58 mRNA. The increase in DDX58 is most pronounced after the knockout of ALKBH5, which also significantly enriches RIG-I-like receptor and IFN-α/β signals[35]. We analyzed the TCGA database. It was found that ALKBH5 showed high expression in the low-expression group of IFI27, and IFI27 was highly induced by IFN-α. Based on existing research evidence, we speculate that down-regulation of ALKBH5 in HNSCC may promote the production of IFI27 through the RIG-I/IFN-α axis.

In summary, our findings indicate that IFI27, acting as an oncogene, is significantly associated with poor survival in a variety of tumors, and is closely related to the poor prognosis of HNSCC. Within the tumor microenvironment, IFI27 facilitates cancer cell proliferation, potentially through regulation by the ALKBH5/RIG-I/IFN-α axis. Furthermore, IFI27 exacerbates HNSCC progression by negatively modulating innate immune responses and inducing EMT, suggesting its potential as a novel therapeutic target for HNSCC. This study utilized bioinformatics analysis and immunohistochemistry to investigate the expression and mechanisms of IFI27 in HNSCC based on data from the TCGA database and multiple online platforms. Despite achieving notable progress, the results are constrained by the limited sample size. Nonetheless, we posit that IFI27 may serve as a prognostic marker for HNSCC. Future research will focus on expanding sample sizes and conducting comprehensive cellular and animal studies to further validate these findings.

Methods

Data collection of TCGA and clinical cases

We downloaded gene expression data and clinicopathological information of HNSCC patients from the TCGA official website (https://portal.gdc.cancer.gov/). We removed duplicate samples and excluded cases lacking clinical information. This resulted in a total of 409 tumor tissues and 43 paracancerous tissues available for further analysis.

We collected 57 surgical resection paraffin-embedded tissue specimens from the pathology department of our hospital between January 2018 and October 2022. In addition, 20 paracancer specimens (tissues 2 cm away from the surrounding cancer tissues, which were confirmed as normal tissues by HE staining) were taken as controls. All patients were diagnosed with HNSCC in the oral and maxillofacial surgery department of our hospital and underwent surgical treatment without preoperative radiotherapy, chemotherapy, immunotherapy, targeted therapy, or other forms of therapy. The collected clinicopathological features included gender, age, lymph node metastasis, TNM stage (American Joint Committee on Cancer (AJCC), 8th Edition), and tumor differentiation. Follow-up information was obtained from patients' medical records or by contacting the patients and their families.

Immunohistochemistry (IHC) experiments

The experimental reagents included the IFI27 antibody (diluted 1:100, Affinity, DF8989), ALKBH5 antibody (diluted 1:100, Wuhan Sanying Biotechnology Co., Ltd., 67811-1-Ig), diaminobenzidine (DAB) chromogenic reagent, hematoxylin staining solution, 5% bovine serum albumin, absolute ethanol, xylene, and neutral gum.

The paraffin-embedded tissue blocks were sliced and deparaffinized in xylene until fully hydrated. The sections were placed in citrate buffer under high pressure, and endogenous peroxidase was blocked. A 5% bovine serum albumin solution was used for blocking. Primary antibodies, including the IFI27 antibody and ALKBH5 antibody, were added and incubated overnight. Subsequently, the secondary antibody and diaminobenzidine were added for color development, followed by hematoxylin redyeing and dehydration sealing.

The number of positive immunostained cells and total cells were determined through human-computer interaction, with nuclei stained blue and positive staining appearing brown or tan. Positive results were interpreted using a semi-quantitative integral method. The color development intensity scores were defined as follows: 0 for no color, 1 for light yellow, 2 for tan, and 3 for brown. According to the percentage of positive cells observed under the microscope, scores were assigned as follows: 1 for < 10%, 2 for 10–50%, 3 for 51–80%, and 4 for > 80%. The semi-quantitative immune response score was calculated by multiplying the color development

intensity by the percentage of positive cells. Scores of 0–4 were classified into the low-expression group ($n = 26$), while scores of 6–12 were classified into the high-expression group ($n = 31$).

HE staining experiments

The slices were placed in a 70 °C in situ hybridization apparatus and baked for 30 min; Quickly added the baked slices into the xylene and repeated twice for 5 min each time; Then, placed them in 100%, 90%, 80%, 70% ethanol for 5 min, and in distilled water for 5 min; Blotted the water, added hematoxylin dye solution, stained for 5 min, rinsed off the hematoxylin dye solution with running water, and observed the staining degree with a microscope; Differentiated with 1% hydrochloric acid alcohol for 1∼3 s, washed and immersed in ammonia water for 5∼10 min, then washed, microscope observed color; Added 0.5% eosin dye 1 drop, stained for 1 min, and then observed with microscope after cleaning with distilled water; The slices were dehydrated with 80%, 90%, 95% and 100% ethanol; Placed them in xylene twice for 5 min each time, dried at room temperature; Added a drop of neutral gum to the tissue, covered the glass to seal the film, and placed them under a microscope for observing and photographing 24h later.

Blue: normal nuclei are bright blue, apoptotic nuclei are blue-black, necrotic cells are light blue or blue disappear, cartilage matrix, calcium salt particles are dark blue, mucus is gray blue. Red: The cytoplasm is pink to pink in different shades, the intracytoplasmic eosinophilic granules are bright red, the collagen fibers are light pink, the elastic fibers are bright pink, the erythrocytes are orange, and the protein fluid is pink.

Bioinformatics analysis

In this study, the GENE_DE module based on the Exploration of TIMER 2.0 (http://timer.cistrome.org/) database was used to observe the expression of IFI27 in a variety of cancers. The Expression module of the TCGA Gene based on the UALCAN database (http://ualcan.path.uab.edu/) was used to compare the correlation between the expression level of IFI27 and various clinicopathological features of HNSCC patients. The Methylation module was also used to analyze the methylation levels of the IFI27 promoter in both HNSCC tumor and normal tissues. The choice to use tools like TIMER 2.0 and UALCAN for analysis was based on their respective functions and advantages. TIMER 2.0 utilized data from public databases such as TCGA, ensuring the reliability and broad applicability of its analysis results. It supported the analysis of various cancer types and was widely used in research across different tumor types. UALCAN offered multiple features, such as gene expression differential analysis, mutation analysis, and clinical correlation analysis, helping researchers explore the relationship between gene expression data and cancer progression in depth. The expression values of IFI27 were analyzed in 409 TCGA patients and 57 clinical cases. The median expression value was used as a cutoff to divide the patients into two groups: the IFI27 high-expression group ($n = 205$) and the IFI27 low-expression group ($n = 204$). Survival analysis and visualization were performed using the R packages "survival" and "survminer". Pearson correlation analysis identified 150 genes positively associated with IFI27 in the TCGA database ($P < 0.05$). The R package "org.Hs.eg.db" (version: 3.18.0) was then used to convert these genes into ENTREZID. GSEA was performed on the DEGs of IFI27 using the gene set (h.all.v2023.2.Hs.symbols.gmt) from the Molecular Signatures Database (https://www.gseamsigdb.org/). A gene set was considered significantly enriched when p.adjust < 0.05. The differential expression of 23 m6A modification-related regulators was compared between the IFI27 high-expression group and the low-expression group, and explored the relationship between IFI27 and ALKBH5.

Statistical analysis

We processed the data using IBM SPSS Statistics 27.0 for statistical analysis. We employed the Wilcoxon rank sum test to assess the significance of differences between two groups with non-normal distributions. Additionally, the Chi-square test was used to compare the expression of IFI27 across various clinicopathological feature groups. KM curves were utilized to establish a prognostic model, while Cox regression analysis was conducted to investigate prognostic factors, considering $P < 0.05$ as statistically significant.

Data availability

All data generated or analyzed during this study are included in this article.

Received: 30 October 2024; Accepted: 14 February 2025
Published online: 24 February 2025

References

1. Chen, S. M. Y. et al. Tumor immune microenvironment in head and neck cancers. *Mol. Carcinog.* **59** (7), 766–774. https://doi.org/10.1002/mc.23162 (2020).
2. Sim, F., Leidner, R. & Bell, R. B. Immunotherapy for head and neck cancer. *Oral Maxillofac. Surg. Clin. North. Am.* **31**(1), 85–100. https://doi.org/10.1016/j.coms.2018.09.002 (2019).
3. Djureinovic, D., Wang, M. & Kluger, H. M. Agonistic CD40 antibodies in cancer treatment. *Cancers* **13**(6), 1302. https://doi.org/10.3390/cancers13061302 (2021).
4. Johnson, D. E. et al. Head and neck squamous cell carcinoma. *Nat. Rev. Dis. Primers* **6**(1), 92. https://doi.org/10.1038/s41572-020-00224-3 (2020).
5. Manne, S. L. et al. Self-efficacy in managing post-treatment care among oral and oropharyngeal cancer survivors. *Eur. J. Cancer Care (Engl.)* **31**(6), e13710. https://doi.org/10.1111/ecc.13710 (2022).
6. Schneider, W. M., Chevillotte, M. D. & Rice, C. M. Interferon-stimulated genes: a complex web of host defenses. *Annu. Rev. Immunol.* **32**, 513–545. https://doi.org/10.1146/annurev-immunol-032713-120231 (2014).
7. Suomela, S., Cao, L., Bowcock, A. & Saarialho-Kere, U. Interferon alpha-inducible protein 27 (IFI27) is upregulated in psoriatic skin and certain epithelial cancers. *J. Invest. Dermatol.* **122**(3), 717–721. https://doi.org/10.1111/j.0022-202X.2004.22322.x (2004).
8. Cheriyath, V., Leaman, D. W. & Borden, E. C. Emerging roles of FAM14 family members (G1P3/ISG 6–16 and ISG12/IFI27) in innate immunity and cancer. *J. Interferon Cytokine Res.* **31**(1), 173–181. https://doi.org/10.1089/jir.2010.0105 (2011).

9. Cui, X. et al. IFI27 integrates succinate and fatty acid oxidation to promote adipocyte thermogenic adaption. *Adv. Sci. (Weinh.)* **10**(28), e2301855. https://doi.org/10.1002/advs.202301855 (2023).
10. Gjermandsen, I. M., Justesen, J. & Martensen, P. M. The interferon-induced gene ISG12 is regulated by various cytokines as the gene 6–16 in human cell lines. *Cytokine* **12**(3), 233–238. https://doi.org/10.1006/cyto.1999.0549 (2000).
11. Gao, J. et al. IFI27 may predict and evaluate the severity of respiratory syncytial virus infection in preterm infants. *Hereditas* **158**(1), 3. https://doi.org/10.1186/s41065-020-00167-5 (2021).
12. Edupuganti, R. R. et al. N6-methyladenosine (m6A) recruits and repels proteins to regulate mRNA homeostasis. *Nat. Struct. Mol. Biol.* **24**(10), 870–878. https://doi.org/10.1038/nsmb.3462 (2017).
13. Zhai, Y. & Zheng, L. m6A RNA methylation regulator-related signatures exhibit good prognosis prediction ability for head and neck squamous cell carcinoma. *Sci. Rep.* **12**(1), 16358. https://doi.org/10.1038/s41598-022-20873-6 (2022).
14. Uddin, M. B., Wang, Z. & Yang, C. The m6A RNA methylation regulates oncogenic signaling pathways driving cell malignant transformation and carcinogenesis. *Mol. Cancer* **20**(1), 61. https://doi.org/10.1186/s12943-021-01356-0 (2021).
15. Wei, C. et al. Pan-cancer analysis shows that ALKBH5 is a potential prognostic and immunotherapeutic biomarker for multiple Cancer types including gliomas. *Front. Immunol.* **13**, 849592. https://doi.org/10.3389/fimmu.2022.849592 (2022).
16. Guo, X. et al. R. RNA demethylase ALKBH5 prevents pancreatic cancer progression by posttranscriptional activation of PER1 in an m6A-YTHDF2-dependent manner. *Mol. Cancer* **19**(1), 91. https://doi.org/10.1186/s12943-020-01158-w (2020).
17. Hu, Y. et al. Demethylase ALKBH5 suppresses invasion of gastric cancer via PKMYT1 m6A modification. *Mol. Cancer* **21**(1), 34. https://doi.org/10.1186/s12943-022-01522-y (2022).
18. Jin, D. et al. m6A demethylase ALKBH5 inhibits tumor growth and metastasis by reducing YTHDFs-mediated YAP expression and inhibiting miR-107/LATS2-mediated YAP activity in NSCLC. *Mol. Cancer* **19**(1), 40. https://doi.org/10.1186/s12943-020-01161-1 (2020).
19. Kanehisa, M. & Goto, S. KEGG: Kyoto Encyclopedia of genes and genomes. *Nucleic Acids Res.* **28**, 27–30. https://doi.org/10.1093/nar/28.1.27 (2000).
20. Kanehisa, M. Toward understanding the origin and evolution of cellular organisms. *Protein Sci.* **28**, 1947–1951. https://doi.org/10.1002/pro.3715 (2019).
21. Kanehisa, M., Furumichi, M., Sato, Y., Kawashima, M. & Ishiguro-Watanabe, M. KEGG for taxonomy-based analysis of pathways and genomes. *Nucleic Acids Res.* **51**, D587–D592. https://doi.org/10.1093/nar/gkac963 (2023).
22. Blot, W. J. et al. Jr. Smoking and drinking in relation to oral and pharyngeal cancer. *Cancer Res.* **48**(11), 3282–3287 (1988). https://pubmed.ncbi.nlm.nih.gov/3365707/
23. Hennessey, P. T., Westra, W. H. & Califano, J. A. Human papillomavirus and head and neck squamous cell carcinoma: recent evidence and clinical implications. *J. Dent. Res.* **88**(4), 300–306. https://doi.org/10.1177/0022034509333371 (2009).
24. Tsang, C. M., Lui, V. W. Y., Bruce, J. P., Pugh, T. J. & Lo, K. W. Translational genomics of nasopharyngeal cancer. *Semin Cancer Biol.* **61**, 84–100. https://doi.org/10.1016/j.semcancer.2019.09.006 (2020).
25. Velleuer, E. & Dietrich, R. Fanconi anemia: young patients at high risk for squamous cell carcinoma. *Mol. Cell. Pediatr.* **1**(1), 9. https://doi.org/10.1186/s40348-014-0009-8 (2014).
26. Adelstein, D. et al. NCCN guidelines insights: Head and Neck cancers, Version 2.2017. *J. Natl. Compr. Canc Netw.* **15**(6), 761–770. https://doi.org/10.6004/jnccn.2017.0101 (2017).
27. Paludan, S. R. & Bowie, A. G. Immune sensing of DNA. *Immunity* **38**(5), 870–880. https://doi.org/10.1016/j.immuni.2013.05.004 (2013).
28. Fucikova, J. et al. Prognostic and predictive value of DAMPs and DAMP-Associated processes in Cancer. *Front. Immunol.* **6**, 402. https://doi.org/10.3389/fimmu.2015.00402 (2015).
29. Liu, Y., Liu, Y. L. & Ge, S. X. Research progress towards interferon stimulated genes and its clinical significance. *Chin. J. Immunol.* **34**(03), 454–459. https://doi.org/10.3969/j.issn.1000-484X.2018.03.028 (2018).
30. Heyn, H. & Esteller, M. DNA methylation profiling in the clinic: applications and challenges. *Nat. Rev. Genet.* **13**(10), 679–692. https://doi.org/10.1038/nrg3270 (2012).
31. Villamayor, L. et al. The IFN-stimulated gene IFI27 counteracts innate immune responses after viral infections by interfering with RIG-I signaling. *Front. Microbiol.* **14**, 1176177. https://doi.org/10.3389/fmicb.2023.1176177 (2023).
32. Li, S. et al. Interferon alpha-inducible protein 27 promotes epithelial-mesenchymal transition and induces ovarian tumorigenicity and stemness. *J. Surg. Res.* **193**(1), 255–264. https://doi.org/10.1016/j.jss.2014.06.055 (2015).
33. Chiang, K. C. et al. Interferon α-inducible protein 27 is an oncogene and highly expressed in cholangiocarcinoma patients with poor survival. *Cancer Manag. Res.* **11**, 1893–1905. https://doi.org/10.2147/CMAR.S196485 (2019).
34. Huang, S. et al. Interferon alpha-inducible protein 27 (IFI27) is a prognostic marker for pancreatic cancer based on comprehensive bioinformatics analysis. *Bioengineered* **12**(1), 8515–8528. https://doi.org/10.1080/21655979.2021.1985858 (2021).
35. Jin, S. et al. The m6A demethylase ALKBH5 promotes tumor progression by inhibiting RIG-I expression and interferon alpha production through the IKKε/TBK1/IRF3 pathway in head and neck squamous cell carcinoma. *Mol. Cancer* **21**(1), 97. https://doi.org/10.1186/s12943-022-01572-2 (2022).

Author contributions

C.W. and S.Z. have made substantial contributions to the conception and design of the study, and integrated the manuscript. Z.C. and S.Z. provided guidance on the methodology of the article and revised the manuscript. C.W., T.L., Y.B. and J.G. conducted literature collection and summary. S.Z. is the corresponding authors for this manuscript. All authors have read and agreed to the published version of the manuscript.

Competing interests

The authors declare no competing interests.

Ethics approval

All procedures were performed in accordance with the 1964 Helsinki Declaration and its later amendments or comparable ethical standards. This study was approved by the institutional review board (IRB) of the Fourth Hospital of Hebei Medical University (IRB No.2025KS012). The need for informed consent was waived under the approval of the IRB of the Fourth Hospital of Hebei Medical University due to the retrospective design of the study.

Additional information

Correspondence and requests for materials should be addressed to S.Z.

Reprints and permissions information is available at www.nature.com/reprints.